

Electromagnetic Radiation Trapped in the Magnetosphere above the Plasma Frequency

DONALD A. GURNETT AND ROBERT R. SHAW

*Department of Physics and Astronomy
University of Iowa, Iowa City, Iowa 52242*

An electromagnetic noise band is frequently observed in the outer magnetosphere by the Imp 6 spacecraft at frequencies from about 5 to 20 kHz. This noise band generally extends throughout the region from near the plasmopause boundary to near the magnetopause boundary. The noise typically has a broadband field strength of about $5 \mu\text{V m}^{-1}$. The noise band often has a sharp lower cutoff frequency at about 5 to 10 kHz, and this cutoff has been identified as the local electron plasma frequency. Since the plasma frequency in the plasmasphere and solar wind is usually above 20 kHz, it is concluded that this noise must be trapped in the low-density region between the plasmopause and magnetopause boundaries. The noise bands often contain a harmonic frequency structure which suggests that the radiation is associated with harmonics of the electron cyclotron frequency. The frequency spacing of these harmonics does not, however, appear to be related to the local electron cyclotron frequency. Possible mechanisms that could explain the generation of this noise are discussed.

An electromagnetic noise band is consistently observed above the local electron plasma frequency in the outer magnetosphere with the University of Iowa plasma wave experiment on the Imp 6 spacecraft. This noise band usually extends throughout the region from the plasmopause boundary to the magnetopause boundary. The frequency range of the noise band is typically about 5 to 20 kHz. The lower cutoff frequency of the noise band is often very sharply defined and is believed to be caused by the ordinary mode propagation cutoff at the local electron plasma frequency. Since the plasma frequency in the plasmasphere and solar wind is usually above 20 kHz, this noise must be trapped in the low-density region between the plasmopause and magnetopause boundaries. The intensity of the noise band is usually very low, typically about $5 \mu\text{V m}^{-1}$ broadband intensity, and probably could not be detected without using long electric antennas of the type used on Imp 6. This noise does not appear to be associated with the 'high-pass' noise reported by *Dunckel et al.* [1970] and *Stone et al.* [1971], and to our knowledge has not been previously identified, probably because of the very low intensity. The purpose of this paper is to describe the characteristics of the trapped electromag-

netic noise detected by Imp 6 above the electron plasma frequency and to discuss the propagation and origin of this noise.

DESCRIPTION OF INSTRUMENTATION

The Imp 6 spacecraft was launched on March 13, 1971, into a highly eccentric earth orbit with initial perigee and apogee geocentric radial distances of 6613 km and 212,630 km, respectively, orbit inclination of 28.7 deg, and period of 4.18 days. This orbit carries Imp 6 through most of the major regions of the magnetosphere and into the solar wind. Imp 6 is a spin-stabilized spacecraft with the spin axis oriented approximately perpendicular to the ecliptic plane and a nominal rotation period of about 11 sec.

The University of Iowa plasma wave experiment on Imp 6 detects plasma wave phenomena in the frequency range from 20 Hz to 200 kHz. The antennas for this experiment consist of three mutually orthogonal 'long-wire' dipole antennas for electric field measurements and three mutually orthogonal loop antennas for magnetic field measurements. Two of the electric dipole antennas are perpendicular to the spacecraft spin axis. These antennas, E_x and E_y , have tip-to-tip lengths of 53.5 meters and 92.5 meters, respectively. The E_z antenna, which lies along the spin axis, has a tip-to-tip length of 7.7

meters. Any of the six antennas can be connected to either of two identical spectrum analyzers and two wideband receivers.

Each of the two spectrum analyzers consists of sixteen channels with center frequencies from 36 Hz to 178 kHz. The filter for each channel has a bandwidth of approximately 15% of the center frequency, and there are four filters per decade of frequency. Each frequency channel has two detectors, a peak detector and an average detector. The peak detector has a response time constant of 0.1 sec and measures the largest signal occurring in a given sample interval (5.11 sec), and the average detector measures the average noise intensity, with a time constant of 5.11 sec, during each sample interval. In addition to the peak and average detectors, the 36-Hz, 311-Hz, 3.11-kHz, and 31.1-kHz channels also have a rapid sample detector output. The time constant of this detector is 0.1 sec and it is sampled every 0.32 sec. The telemetered output of each detector is a voltage proportional to the logarithm of the quantity being measured. The dynamic range of each spectrum analyzer channel is 100 db.

The spectrum analyzer channels each have an rms sensitivity of about $10 \mu\text{v}$ for a sine wave signal. When connected to one of the long electric dipole antennas, this sensitivity permits measurements of electric field strengths as low as $0.2 \mu\text{v m}^{-1}$ in each frequency channel. The corresponding magnetic field sensitivity of the loop antenna is a function of frequency and varies from about $2.0 \text{ m}\gamma$ at 36 Hz to about $10.0 \mu\gamma$ at 16.5 kHz.

In conjunction with the two spectrum analyzers, the University of Iowa plasma wave experiment includes two wideband receivers. These receivers are automatic gain control receivers and provide broadband coverage of the frequency ranges from 10 Hz to 1 kHz and from 650 Hz to 30 kHz, depending on the particular mode of operation selected. The analog signals from the wideband receivers are transmitted to the ground via the special purpose analog transmitter. These wideband signals are used for high-frequency-time resolution analysis of transient and narrow band wave phenomena.

CHARACTERISTICS OF THE TRAPPED $f > f_p$ NOISE BAND

The spectrum analyzer data for an outbound Imp 6 pass through the magnetosphere, from about 2.6 to 16.0 R_E geocentric radial distance, near local noon are shown in Figure 1. The data plotted are the raw voltage outputs of the spectrum analyzer connected to the E_v electric antenna. The ordinate for each frequency channel is proportional to the logarithm of the electric field strength in that channel. The interval from the baseline of one channel to the baseline of the next higher channel represents a dynamic range of 100 db. The vertical bars for each of the sixteen frequency channels represent the electric field strength averaged over a time interval of 81.8 sec. The dot above each of the vertical bars is the largest peak field strength seen over the same 81.8-sec time interval.

The enhanced signal strength in the four lowest frequency channels, particularly in the peak measurement, is caused by voltage transients in the spacecraft solar array produced as the shadow of the loop antenna passes over the solar cells. The magnitude of this interference depends on several factors, the most important of which is the electron density. This dependence provides a useful method of identifying the plasmopause boundary from the abrupt increase in the interference level as the spacecraft passes from the high-density region inside the plasmasphere to the low-density region outside. The abrupt increase in the solar array interference evident at about 0650 UT in the 36-, 63-, 120-, and 200-Hz channels of Figure 1 provides a clear indication that the spacecraft crossed the plasmopause at this time.

Essentially coincident with the plasmopause crossing, a noise band, indicated by a dashed line in Figure 1, can be seen sweeping downward in frequency through the 178-, 100-, 56.2-, 31.1-, and 16.5-kHz channels as the spacecraft proceeds outward to larger radial distances. This noise band is frequently found in the Imp 6 electric field data near the plasmopause. Because of the distinctive frequency variation at the plasmopause boundary, abruptly decreasing in frequency as the electron density decreases, we believe that this noise band is associated with the upper hybrid resonance (UHR) frequency

GURNETT AND SHAW: TRAPPED EM RADIATION

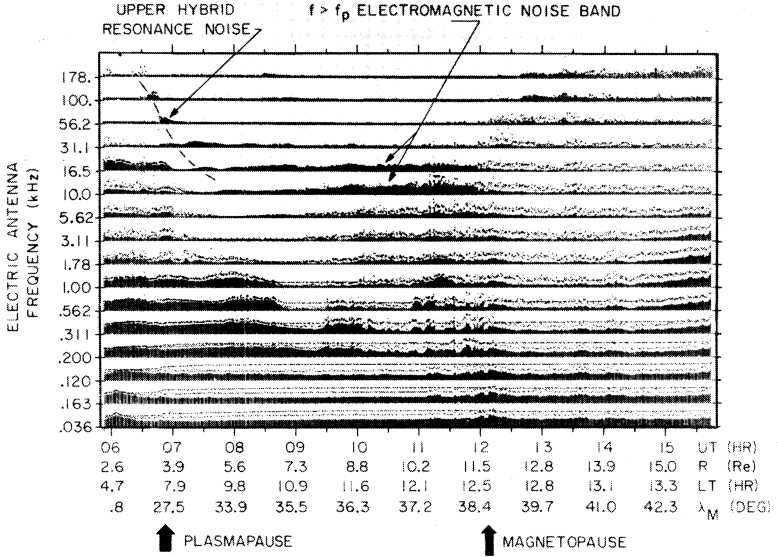


Fig. 1. An outbound Imp 6 pass (orbit 79, January 31, 1972) near local noon showing an upper hybrid resonance noise band near the plasmopause boundary and an electromagnetic noise band above the plasma frequency ($f > f_p$) in the region between the plasmopause and magnetopause boundaries. Note the abrupt termination of the $f > f_p$ noise band at the magnetopause.

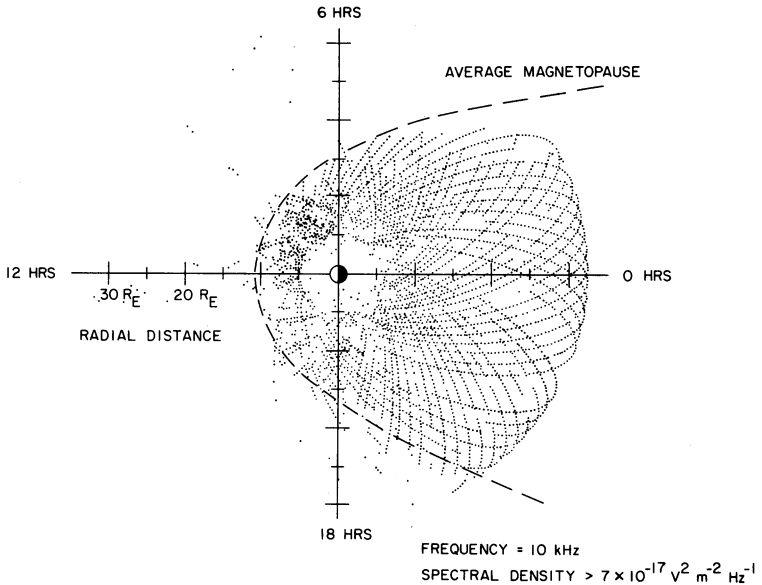


Fig. 2. Region of occurrence of the trapped $f > f_p$ electromagnetic noise as determined from the 10-kHz electric field spectrum analyzer channel. The coordinates are geocentric radial distance and local time. In order to prevent whistlers and other impulsive noise phenomena from contributing to this survey, only field strengths with a peak to average ratio less than 1.2 are included.

$$f_{UHR} = (f_p^2 + f_g^2)^{1/2} \quad (1)$$

where f_p is the electron plasma frequency (proportional to the square root of the electron density) and f_g is the electron gyrofrequency [Stix, 1962]. Quantitative estimates of the expected UHR frequency near the plasmopause boundary indicate that this identification is reasonable. Similar noise bands associated with the UHR frequency have been observed at lower altitudes in the plasmasphere and ionosphere by numerous rocket- and satellite-borne radio noise experiments [Walsh *et al.*, 1964; Bauer and Stone, 1968; Gregory, 1969; Muldrew, 1970; Hartz, 1970], as well as by the GSFC radio astronomy experiment on Imp 6 [Mosier *et al.*, 1973].

A second noise band is also evident in the 10.0- and 16.5-kHz channels of Figure 1 in the region between the plasmopause and magnetopause boundaries. This noise band terminates abruptly at the magnetopause boundary. Near the plasmopause boundary this noise band appears to be above the UHR-related noise band. As we will show later, this second noise band is completely separate from the UHR noise band and consists of electromagnetic waves propagating at frequencies above the local electron plasma frequency.

Electromagnetic noise bands of the type illustrated in Figure 1 are observed at essentially all local times in the region between the plasmopause and magnetopause boundaries. Figure 2 shows the spatial distribution of this noise as determined from the Imp 6 electric field data. The local time and radial distance coordinates plotted represent points at which the electric field spectral density at 10 kHz exceeds $7 \times 10^{-17} \text{ v}^2 \text{ m}^{-2} \text{ Hz}^{-1}$ and the ratio of the peak to the average electric field strength is less than 1.2. These criteria for identifying the noise are based on a qualitative survey of electric field intensity plots of the type shown in Figure 1 for the first year of inflight data. This survey indicated that when the noise is present it is nearly always detectable in the 10-kHz electric field channel and that the noise intensity usually varies relatively slowly on a time scale of 10 sec or less (peak to average field intensity less than 1.2). The peak to average intensity criterion used for identifying this noise is necessary to eliminate certain other types of impulsive

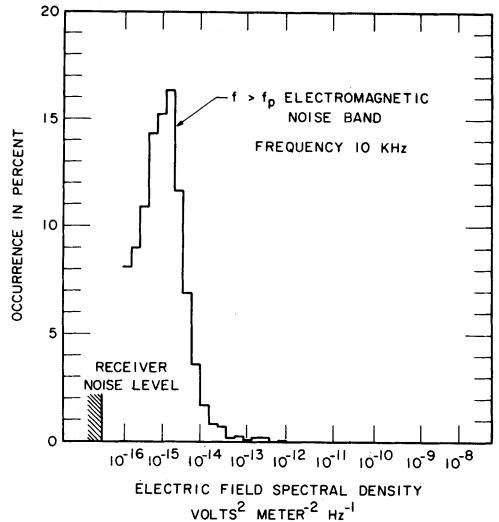


Fig. 3. Distribution of electric field intensities for the $f > f_p$ noise band at 10 kHz. This distribution summarizes about 1500 measurements obtained over a 1-yr period. Again only field strengths with a peak to average ratio less than 1.2 are included.

noise, such as occur in the bow shock and in the magnetosheath, which would otherwise contribute to the spatial survey. The threshold electric field spectral density in Figure 2 and all subsequent electric field intensities given in this paper are computed by assuming that the effective length of the electric antenna is one-half of the tip-to-tip length and that the antenna impedance is small compared to the base loading impedance. In order to provide an unbiased representation of the region of occurrence, the time interval between the points in Figure 2 is normalized to provide a constant number of points per unit length along the spacecraft trajectory. The data in Figure 2 represent one complete year of operation, thereby assuring coverage of all local times, with the exception of two orbits at about 2200 LT, for which correct orbit parameters are not currently available.

The spatial survey in Figure 2 shows that the $f > f_p$ noise band is observed almost continuously throughout the region between the plasmopause and magnetopause boundaries. The cutoff at the magnetopause boundary is clearly evident, and the position of this cutoff agrees well with the average magnetopause location given by Fairfield [1971]. The inner

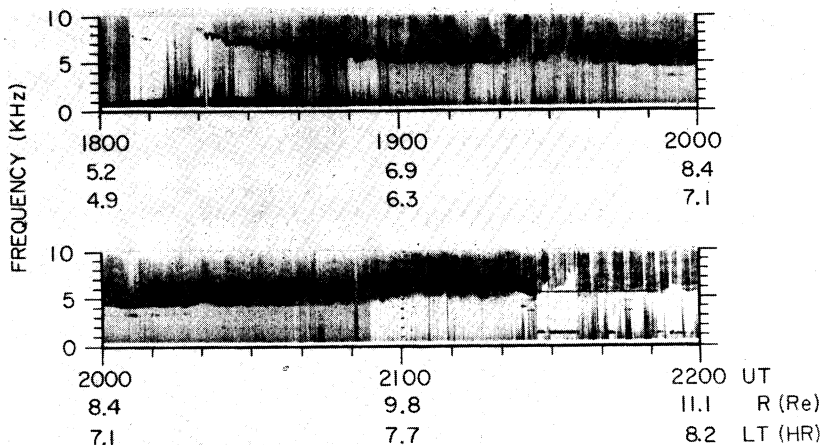


Fig. 4. Electric field frequency-time spectrogram showing the sharp lower cutoff frequency of the trapped $f > f_p$ noise band (Imp 6 orbit 95, April 6, 1972). The lower cutoff of the noise band is at the local electron plasma frequency f_p .

boundary at about $4 R_E$ agrees reasonably well with the expected location of the plasmopause boundary. In contrast to many other types of noise found in the magnetosphere, the intensity of the $f > f_p$ noise band is remarkably constant from orbit to orbit. Figure 3 shows the distribution of electric field intensities of the $f > f_p$ noise at 10 kHz as obtained from about 1500

measurements distributed over one year of operation. The data points used to calculate this distribution are selected at uniform spatial intervals along the spacecraft trajectory, comparable to the spacing between the data points in Figure 2, and only field strengths that have a ratio of peak to average field strengths less than 1.2 are counted. The electric field strength distribution in Figure 3 shows that the intensity of the $f > f_p$ noise band is usually confined to the rather narrow range from about 6×10^{-16} to $6 \times 10^{-15} \text{ v}^2 \text{ m}^{-2} \text{ Hz}^{-1}$. No cases were found with an intensity exceeding $10^{-12} \text{ v}^2 \text{ m}^{-2} \text{ Hz}^{-1}$. The threshold intensity of $7 \times 10^{-17} \text{ v}^2 \text{ m}^{-2} \text{ Hz}^{-1}$ used in the spatial survey of Figure 2 is sufficiently low that essentially all regions where the $f > f_p$ noise band occurs should be included in this survey. Similar spatial surveys with higher thresholds show that the electric field strength is relatively uniform within the primary region of occurrence and has no pronounced variation with radial distance, out to $\sim 32 R_E$ in the tail, or with local time.

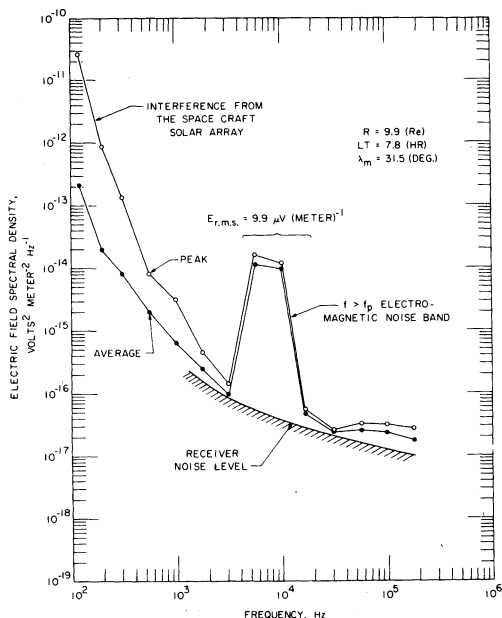


Fig. 5. Electric field spectral density at 21h 04m 30s UT for the pass shown in Figure 4 (orbit 95, April 6, 1972).

A high-resolution frequency-time spectrogram of the wideband electric field data obtained for a pass through the local dawn region is shown in Figure 4 to illustrate the detailed spectral characteristics of the $f > f_p$ noise band. The noise band is seen to have a sharply defined lower cutoff frequency which changes systematically as the spacecraft moves outward to larger radial distances. The lower cutoff frequency sometimes varies by $\sim 10\%$ on a time scale of a

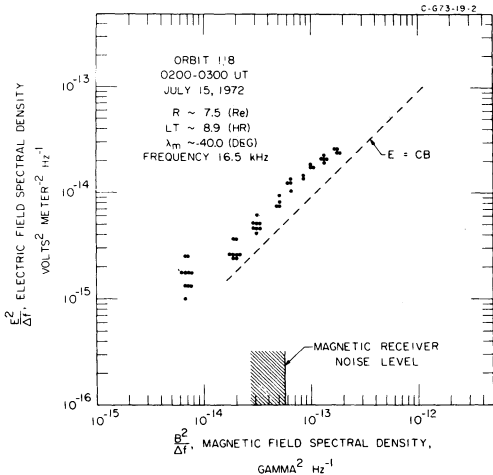


Fig. 6. A series of simultaneously measured electric and magnetic field spectral densities obtained as Imp 6 passes through a trapped $f > f_p$ noise band in the local morning (orbit 118, 0200–0300 UT, July 15, 1972). The magnetic spectral densities have been corrected to eliminate the magnetic receiver noise. The dashed line, $E = cB$, gives the electric to magnetic field ratio for an electromagnetic wave in free space.

few minutes or less. In this case the lower cutoff frequency of the noise band is believed to be at the local electron plasma frequency. The detailed relationship between the observed cutoff frequency of the noise band and the local plasma frequency is discussed in the next section. The electric field spectral density of the $f > f_p$ noise band illustrated in Figure 4 is shown as a function of frequency in Figure 5 at the time 21h 04m 30s UT. The spectral densities in Figure 5 have been computed using the antenna voltage measurements from the 16-channel spectrum analyzer. In this case the maximum electric field spectral density of the noise band is about $10^{-14} \text{ v}^2 \text{ m}^{-2} \text{ Hz}^{-1}$ and the integrated broadband electric field strength is $9.9 \mu\text{v m}^{-1}$.

The slight enhancement of the electric field strength above the receiver noise level in the frequency range from about 30 to 200 kHz in Figure 5 is caused by highpass noise of the type reported by Dunckel *et al.* [1970]. Highpass noise is often evident in the 100- and 178-kHz frequency channels, usually with intensities many orders of magnitude greater than the example in Figure 5, but generally does not appear to be associated with the $f > f_p$ electromagnetic noise band.

Because the loop antenna on Imp 6 has a lower sensitivity to electromagnetic waves than the long electric antenna, and because the intensity of the $f > f_p$ noise band is normally very low, seldom exceeding $10 \mu\text{v m}^{-1}$, it is usually not possible to detect the magnetic field of this noise with the loop antenna. In a few cases, however, the noise band is sufficiently intense that a magnetic field can be clearly detected. One such case is illustrated in Figure 6, which shows a series of simultaneous electric and magnetic field measurements at a frequency of 16.5 kHz as the spacecraft passes through the region between the plasmopause and magnetopause boundaries. Because the magnetic field strength is very weak, the magnetic field intensities shown in Figure 6 are obtained by subtracting the receiver noise level from the measured noise intensity (signal plus noise). The ratio of the electric to magnetic field strengths is also seen to be very close to the free space value of $E = cB$ (shown by the dashed line in Figure 6), as would be expected for electromagnetic waves propagating at frequencies well above the electron plasma frequency. The plasma frequency in this case was about 10 kHz as determined from the lower cutoff frequency of the noise band. The deviation of the measured electric to magnetic field ratio from the free space value can be almost completely accounted for by the decrease in the refractive index, hence increase in the E to B field ratio, due to the presence of the plasma. During each of about 15 magnetospheric passes for which the electric field intensity of the $f > f_p$ noise exceeded about $10^{-14} \text{ v}^2 \text{ m}^2 \text{ Hz}^{-1}$ a corresponding proportional increase has been observed in the magnetic field strength. This close proportionality between the electric and magnetic field strengths provides clear evidence that the $f > f_p$ noise band consists of electromagnetic waves.

IDENTIFICATION OF THE PLASMA FREQUENCY

Although the spectrum analyzer data suggest that the UHR noise band may merge with the $f > f_p$ noise band at the plasmopause boundary, as in Figure 1, the higher resolution wideband data reveal that the $f > f_p$ noise band is not associated with the UHR noise. To illustrate the detailed relationship between these two noise bands, we have selected one particular magnetospheric pass for discussion. This pass

was selected mainly because it shows the spectral characteristic of these noise bands with better than normal clarity. Although this pass probably cannot be considered 'typical,' similar spectral characteristics have been observed on many other passes.

The results obtained from analyzing this selected pass, which is an outbound pass in the local dawn region, are summarized in Figures 7, 8, and 9. Figure 7 shows the spectrum analyzer data obtained near the plasmopause boundary on this pass. The plasmopause is located at about 1533 UT. A noise band, indicated by the dashed lines, is clearly evident in these data sweeping downward in frequency as the spacecraft passes outward through the plasmopause boundary. Because of the similarity to the UHR noise band observations of *Mosier et al.* [1973] inside the plasmopause and the distinctive frequency variation at the plasmopause boundary, we feel that this noise band can be identified, with a high degree of confidence, as the UHR noise band. As soon as the frequency of this noise band drops below 30 kHz very detailed frequency spectrum measurements can be obtained from the wideband telemetry. Figure 8 shows a series of 'snapshots' of the electric field frequency-time spectrum obtained in the region outside the plasmopause boundary. The approximate times at which these 'snapshots' were obtained are shown by the arrows marked *A* through *D* in Figure 9, which summarizes the measured cutoff frequencies of all noise bands encountered during this pass. From these data it is seen that the noise band labeled 'electrostatic noise band' in the spectrograms of Figure 8 connects smoothly with the UHR noise band shown in Figure 7. Sharp nulls occur in the intensity of this noise whenever the electric antenna axis is parallel to the geomagnetic field, as indicated by the arrows in Figure 8. This spin modulation indicates that the electric field of this noise is oriented very nearly perpendicular to the geomagnetic field.

In an initial report, *Shaw and Gurnett* [1972] concluded that the 'electrostatic noise band' in Figure 8 was associated with the UHR frequency of the local plasma in the region outside the plasmopause boundary. This association seemed reasonable since this noise band apparently represents a continuous extension of the

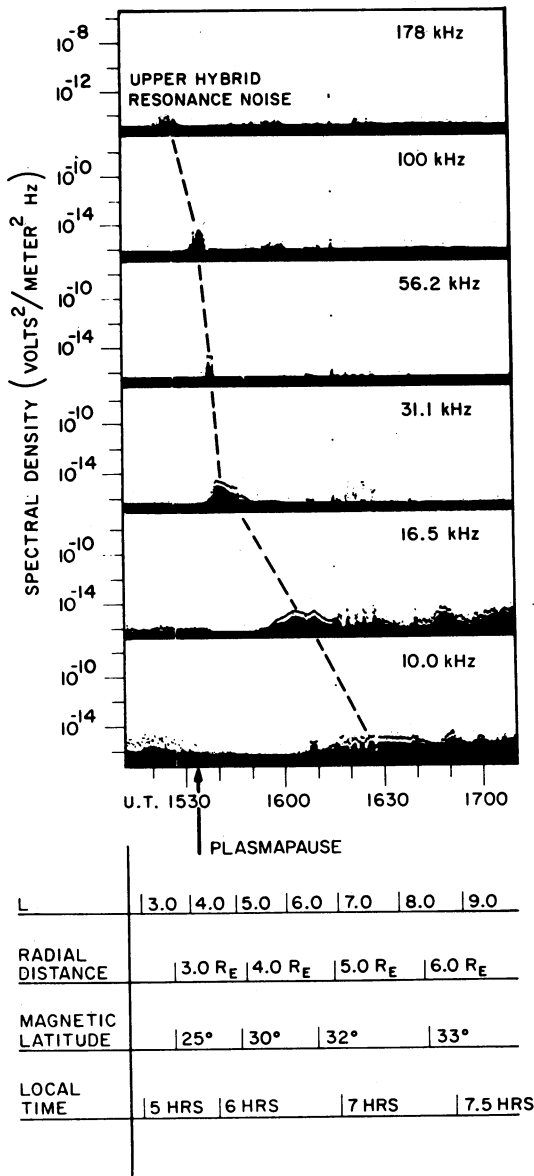


Fig. 7. An example of an upper hybrid resonance noise band observed on an outbound pass through the plasmopause (orbit 7, April 7, 1971).

UHR noise into the region outside of the plasmopause. However, further investigations have revealed that in the region outside the plasmopause this electrostatic noise band cannot be associated with the local UHR frequency. As can be seen in Figure 9, the center frequency of the electrostatic noise band closely follows the electron gyrofrequency throughout the re-

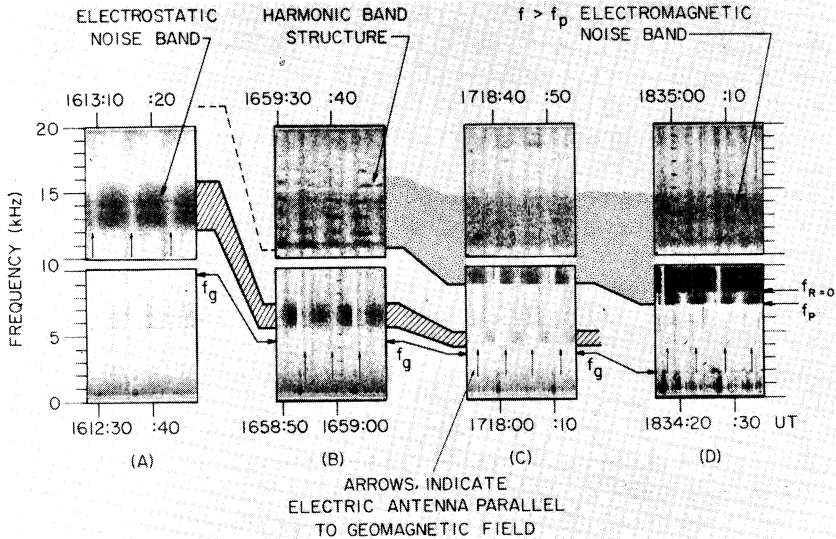


Fig. 8. Selected 'snapshots' of the electric field frequency-time spectrum observed during the outbound pass of Figure 7. Two distinct noise bands are evident. The upper band in (B), (C), and (D) is the trapped $f > f_p$ electromagnetic noise. The electrostatic noise band in (A), (B), and (C) connects with the UHR noise band in Figure 7. Note the two distinct cutoffs, f_p and $f_{R=0}$, evident at the lower edge of the electromagnetic noise band in (D).

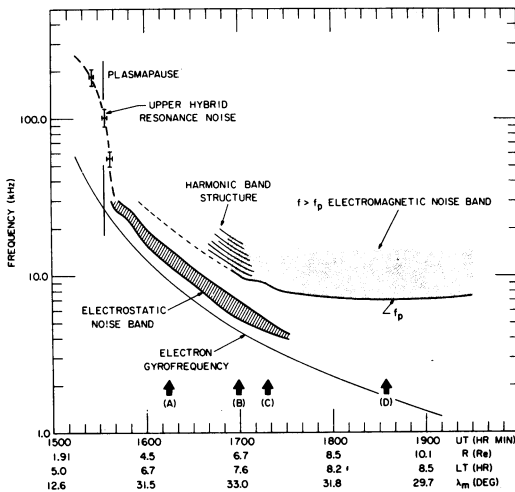


Fig. 9. Summary of all noise band cutoff frequencies observed during the outbound pass illustrated in Figures 7 and 8. Although the upper hybrid resonance (UHR) noise band observed inside the plasmapause is believed to be at the local UHR frequency, this same noise band, when followed outside the plasmapause (labeled electrostatic noise band), is no longer at the local UHR frequency but rather appears to be proportional to the electron gyrofrequency.

gion outside the plasmapause boundary. This type of association with the local electron gyrofrequency is frequently observed in the region beyond the plasmapause. In a few cases electrostatic noise bands of the type shown in Figure 8 have been observed to merge into an intense narrow band electrostatic emission at $\sim (3/2)f_o$, similar to the $(n + 1/2)f_o$ electrostatic emissions discussed by Kennel *et al.* [1970]. Since it is very unlikely that the plasma density varies in such a way that the UHR frequency is proportional to the electron gyrofrequency, this relationship strongly indicates that the electrostatic noise band is not associated with the UHR frequency, at least in the region outside the plasmapause. Simultaneous nonthermal electron and proton density measurements obtained from the Lepedeia instrumentation on Imp 6 have conclusively verified that the electrostatic noise band in Figure 8 cannot be associated with the UHR frequency (L. A. Frank, personal communication, 1973).

Spectrograms B, C, and D of Figure 8 clearly show the $f > f_p$ noise band above the electrostatic noise band. The frequency limits of the $f > f_p$ noise band are plotted in Figure 9. The upper frequency limit of this noise band is

rather poorly defined, but stays at a nearly constant frequency of about 15 kHz throughout the pass. The $f > f_p$ noise band has the characteristic sharp lower cutoff frequency which varies slowly with the spacecraft position, reaching a minimum frequency of about 7.0 kHz at 1830 UT. During certain parts of this pass two distinct lower cutoff frequencies are evident, as in spectrogram *D* of Figure 8. The noise spectrum between the two lower cutoff frequencies has a pronounced spin modulation. As is shown by the arrows in Figure 8, the spin modulation nulls occur when the electric antenna axis is oriented perpendicular to the geomagnetic field, thereby indicating that the electric field of the noise between the two cutoffs is parallel to the geomagnetic field.

The two distinct lower cutoffs of the $f > f_p$ noise band shown in Figure 8(*D*) are easily explained by cold plasma theory if this noise is propagating at frequencies above the plasma frequency, as has been assumed. As is well known [Budden, 1961; Ratcliffe, 1962; Stix, 1962], two propagation cutoffs occur for electromagnetic waves propagating in a cold plasma at frequencies greater than the electron plasma frequency. The smaller of these two cutoffs is at the plasma frequency f_p . This cutoff is for the left-hand polarized (ordinary) mode of propagation and is called the (*L*, *O*) mode. The larger of these two cutoffs is at a frequency, $f_{R=0}$, given by

$$f_{R=0} = \frac{f_o}{2} + \left[\left(\frac{f_o}{2} \right)^2 + f_p^2 \right]^{1/2} \quad (2)$$

This cutoff is for the right-hand polarized (extraordinary) mode of propagation and is called the (*R*, *X*) mode. If the two lower cutoffs of the noise band in Figure 8(*D*) are assumed to be f_p and $f_{R=0}$, equation 2 can be used to independently calculate the electron gyrofrequency. The cutoff frequencies measured from Figure 8(*D*) are $f_p = 7.0$ kHz and $f_{R=0} = 8.1$ kHz. The electron gyrofrequency computed from (2) using these measured cutoff frequencies is $f_o = 2.2$ kHz. The measured electron gyrofrequency determined at this time is $f_o = 2.1$ kHz, as obtained from the NASA/GSFC magnetometer on Imp 6 (N. F. Ness, personal communication, 1972). This close agreement between the computed and measured electron gyrofrequency

provides excellent confirmation that these observed cutoffs correspond to the propagation cutoffs, f_p and $f_{R=0}$, for the ordinary and extraordinary modes of propagation. The orientation of the electric field, parallel to the geomagnetic field for frequencies between f_p and $f_{R=0}$, is also in agreement with the electric field direction expected for the ordinary mode of propagation if the wave normal direction is perpendicular to the geomagnetic field. In this case the ordinary mode, which is normally right-hand polarized, becomes linearly polarized with the electric field parallel to the static magnetic field.

As has been discussed by Stix [1962] and others, the propagation cutoffs at f_p and $f_{R=0}$ represent a reflection condition for left- and right-hand polarized electromagnetic waves propagating above the plasma frequency. Since the plasma frequency in the region between the plasmopause and magnetopause is usually less than in the solar wind or plasmasphere, electromagnetic waves can be permanently trapped within this region in a manner similar to the trapping of electromagnetic waves in a microwave cavity. A qualitative model illustrating this reflection and trapping of electromagnetic waves in the magnetosphere is shown in Figure 10. The corresponding regions of propagation for the (*L*, *O*) and (*R*, *X*) modes are also shown in the CMA diagrams at the top of Figure 10 in terms of the normalized parameters

$$X = (f_p/f)^2 \quad Y = (f_o/f) \quad (3)$$

commonly used in magnetoionic theory [Ratcliffe, 1962]. Because the index of refraction goes to zero at the cutoff frequency, Snell's law shows that reflection occurs before the cutoff frequency is actually reached. Thus the observed lower cutoff for waves propagating in this region is not necessarily at the cutoff frequency of the local plasma. Only if some waves are incident normal to the planes of stratification will the observed lower cutoff frequencies of the noise band correspond with the true propagation cutoffs of the ambient plasma. The close agreement between the computed and measured cutoff frequencies in cases such as Figure 8(*D*) implies that there is a sufficiently broad distribution of wave normal angles to assure that some of the waves come very close to the actual cutoffs at f_p and $f_{R=0}$ before being

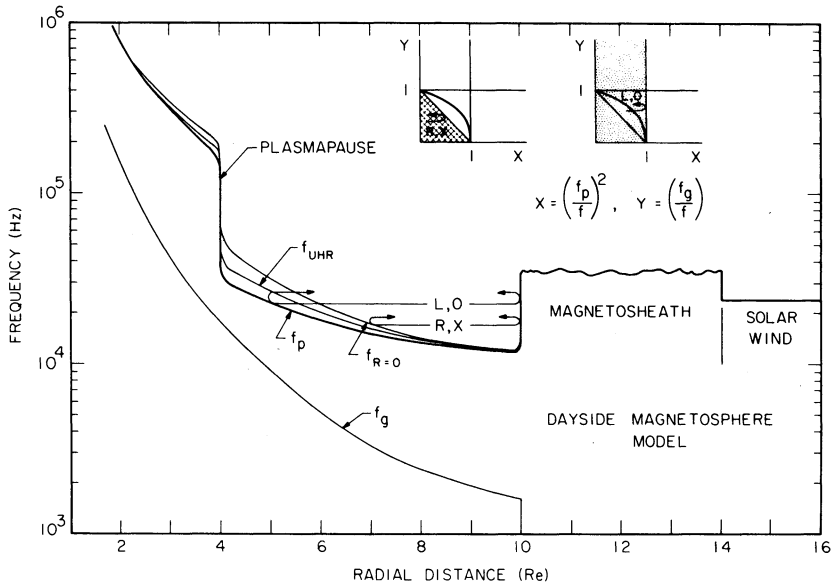


Fig. 10. A magnetospheric model showing the qualitative radial variation of the electron plasma frequency f_p , the upper hybrid resonance frequency f_{UHR} , and the extraordinary mode cutoff $f_{R=0}$. Reflections at f_p and $f_{R=0}$ can trap electromagnetic waves in the low-density region between the plasmapause and magnetopause boundaries.

reflected. If the spatial variation of the plasma frequency is not monotonic, but has hills and valleys, an observed noise band cutoff also may not correspond to the cutoff frequency of the local plasma, since trapped waves may not exist within the valleys of the plasma frequency distribution. In this case a noise band cutoff may be due to a propagation cutoff at some distant location along the ray path. In cases such as Figure 8(D), the occurrence of spin modulation nulls related to the local geomagnetic field guarantees that these noise band cutoffs must be related to cutoff frequencies of the local plasma.

HARMONIC BAND STRUCTURE AND DISCRETE EMISSIONS ABOVE THE PLASMA FREQUENCY

Although the $f > f_p$ noise band usually has a relatively smooth white noise spectrum, this noise does sometimes display certain distinctive frequency-time characteristics. The spectral characteristics are usually of two types: (1) harmonic bands and (2) discrete emissions. The harmonic band structure usually consists of a series of bands, equally spaced in frequency, with a typical frequency separation of about 1 kHz. An example of this harmonic band structure is

clearly evident in Figure 8(B). Another example illustrating this harmonic structure with better detail is shown in Figure 11. Measurements of the frequency interval between the bands indicate that the frequency spacing is not related to the local electron gyrofrequency. For example, the frequency spacing between the bands in Figure 11 is about 1.0 kHz, whereas the measured local electron gyrofrequency is 2.2 kHz. Notice that the noise band in Figure 11 again clearly shows the propagation cutoffs at f_p and $f_{R=0}$. The harmonic bands are often poorly resolved and may fade away and reappear in an irregular pattern, as in the spectrogram of Figure 4. The center frequency of the bands is sometimes very erratic and may change by up to 20% in a time period of a few minutes or less. The spectrogram in Figure 11 shows that the harmonic bands are evident in both the electric and magnetic field data. The close similarity of the electric and magnetic field spectrums indicates that the harmonic structure is due to a frequency-dependent variation of the electromagnetic field intensity rather than a variation in the electric to magnetic field ratio.

Occasionally discrete emissions are observed at frequencies above the local plasma frequency.

sociation, we believe that the discrete emissions in Figure 12 are almost certainly above the local electron plasma frequency. It has not, however, been possible to conclusively identify the location of the f_p or $f_{R=0}$ cutoff frequencies in the region where these emissions are observed. The frequencies of these emissions are much greater than the electron gyrofrequency, which in the region where these data were obtained is only a few kilohertz. Since the discrete emissions are evident in both the electric and magnetic field spectrograms of Figure 12, it is clear that these emissions are electromagnetic waves.

DISCUSSION

The Imp 6 plasma wave experiment has revealed a band of electromagnetic radiation in the frequency range from about 5 to 20 kHz that is essentially always present in the region between the plasmopause and magnetopause boundaries. Substantial evidence has been presented that this noise is propagating at frequencies above the local plasma frequency. Since the plasma frequency in the solar wind and in the plasmasphere is generally greater than 20 kHz, this noise, once generated, must be permanently trapped in the low-density region between the plasmopause and magnetopause boundaries. The intensity of this trapped electromagnetic noise is very low, with broadband electric field strengths seldom exceeding $10 \mu\text{V m}^{-1}$ and power spectral densities of typically $5 \times 10^{-18} \text{ w m}^{-2} \text{ Hz}^{-1}$.

In order to evaluate the mechanisms that could produce this noise, it is necessary to determine the damping, or Q , factor for the electromagnetic radiation trapped within the magnetopause-plasmopause cavity. Since the electron collision frequency in the outer magnetosphere is negligibly small, and since electromagnetic waves propagating at frequencies above the plasma frequency have phase velocities greater than the speed of light, thereby reducing interactions with the thermal plasma, it is expected that these waves would be very weakly damped. Once generated, this radiation may, therefore, undergo many transversals across the cavity, thereby greatly amplifying the observed field strength. The fact that the noise intensity is nearly constant throughout the cavity, apparently independent of the local

plasma regime, provides a strong indication that the radiation must be able to propagate essentially unattenuated over distances on the order of $10 R_E$ or more. The upper cutoff of the noise band corresponds well with the expected solar wind plasma frequency of about 20 kHz, suggesting that this upper cutoff may be due to the greatly enhanced 'leakage' of radiation out of the cavity at frequencies above the solar wind plasma frequency. Because of the unknown plasma density at large radial distances in the geomagnetic tail, it is not known how far this radiation may extend into the geomagnetic tail. However, it is virtually certain that the radiation cannot escape freely out the tail, since the tail cavity would have to extend to distances at which the solar wind plasma frequency is about 5 kHz. This would require that the tail cavity be several AU long, which is much longer than any current estimates of the tail length. Since the radiation must be emitted within the magnetopause-plasmopause cavity, it is entirely possible that the inverse process, absorption, may also be operative in certain regions of the cavity, and this absorption may sharply limit the mean free path of the radiation in these regions.

The presence of harmonically related bands in the frequency spectrum of the trapped $f > f_p$ noise strongly suggests that the emission occurs at or near harmonics of the electron gyrofrequency. The frequency spacing between the bands does not, however, correspond to the local electron gyrofrequency. Assuming that the frequency spacing between the bands does correspond to the electron gyrofrequency at the source, this spacing, which is typically about 1.0 kHz, indicates that the magnetic field in the generation region must be about 30γ . This low value for the magnetic field strength implies that the noise is generated at large radial distances from earth ($>8 R_E$), either near the magnetopause boundary, as Hasegawa [1969] suggested, or in the geomagnetic tail. If the harmonic bands are not related to the electron gyrofrequency but are due to some other unknown effect, then the noise could be generated much closer to the earth. In some cases, such as in Figure 1, the noise can be seen extending up to higher frequencies near the plasmopause boundary, possibly suggesting that the noise is generated near the plasmopause.

Since electromagnetic radiation occurs above the plasma frequency in a wide variety of physical situations, for example in type III solar radio noise bursts [Wild, 1950], in terrestrial kilometric radiation (highpass noise described by Dunckel *et al.* [1970]), and in Jovian decametric radiation [Warwick, 1967], it is of considerable general interest to establish the origin of the magnetospherically trapped $f > f_p$ electromagnetic noise. Two general possibilities can be considered: (1) the noise may be generated by incoherent radiation from energetic electrons within the magnetopause-plasmapause cavity or (2) the noise may be generated by a coherent plasma instability. The only applicable incoherent radiation process is synchrotron radiation, since the radiation must be generated at a frequency that is many times the electron gyrofrequency. Calculations of gyrosynchrotron radiation from electrons in the earth's magnetosphere have been performed by Frankel [1973]; however, because of the uncertainties in the Q of the cavity it is not known whether this mechanism could account for the observed intensities.

Because discrete emissions have been associated with the trapped $f > f_p$ radiation, it seems reasonably certain that a coherent plasma instability must be involved in the generation of some, if not all, of this noise. This instability mechanism clearly must be able to produce electromagnetic radiation at frequencies above the local plasma frequency. Electromagnetic instabilities above the plasma frequency have received relatively little attention in the published literature [Sudan, 1963; Hamasaki, 1968; Gafey *et al.*, 1973] and, as of this time, we do not know of an electromagnetic instability which could directly produce the trapped $f > f_p$ radiation observed by Imp 6. Perhaps future theoretical investigations will establish the existence of such instabilities. If a suitable electromagnetic instability cannot be found, then another possibility is that the noise is produced by coupling from another type of instability. One of the most prominent instabilities at large radial distances in the magnetosphere is the $(n + \frac{1}{2})f_p$ electrostatic cyclotron harmonic emissions discussed by Kennel *et al.* [1970]. These cyclotron harmonic emissions are frequently observed with the high-order harmonics extending to frequencies above the electron plasma frequency,

and the electric field strength of these emissions is typically a factor of 10^2 to 10^3 greater than the field strength of the trapped $f > f_p$ electromagnetic noise. Several mechanisms are known that could couple some of the electrostatic energy into electromagnetic radiation above the plasma frequency. Nonlinear interactions between electrostatic waves can produce electromagnetic radiation, as in the mechanisms proposed by Ginzburg and Zheleznyakov [1958] and Sturrock [1961] to explain type III radio noise bursts. Another possibility is that electromagnetic radiation may be produced by coherent cyclotron radiation from the high-order ($\sim nf_p$) rotating charge distributions associated with the electrostatic electron cyclotron harmonic waves. Further quantitative studies are required to identify which, if any, of these mechanisms are involved in generating the trapped $f > f_p$ electromagnetic noise observed by Imp 6.

Acknowledgments. We wish to thank Dr. L. A. Frank for confirming that the electron densities determined from the electron plasma frequency cutoffs are consistent with the nonthermal electron and proton densities measured by the Lepe-dea instrumentation on Imp 6, and we thank Drs. N. F. Ness and D. H. Fairfield for providing us with the magnetic field data from the NASA/GSFC magnetometer on Imp 6.

This work was supported in part by the National Aeronautics and Space Administration under contract NAS5-11704 and grant NGL-16-001-043 and by the Office of Naval Research under grant N00014-68-A-0196-0003.

* * *

The Editor thanks R. E. Barrington and N. Dunckel for their assistance in evaluating this paper.

REFERENCES

- Bauer, S. J., and R. G. Stone, Satellite observations of radio noise in the magnetosphere, *Nature*, **218**, 1145, 1968.
- Budden, K. G., *Radio Waves in the Ionosphere*, p. 64, Cambridge University Press, London, 1961.
- Dunckel, N., B. Ficklin, L. Rorden, and R. A. Helliwell, Low-frequency noise observed in the distant magnetosphere with Ogo 1, *J. Geophys. Res.*, **75**, 1854, 1970.
- Fairfield, D. H., Average and unusual locations of the earth's magnetopause and bow shock, *J. Geophys. Res.*, **76**, 6700, 1971.
- Frankel, M. S., Gyro-synchrotron radio noise from electrons in the earth's magnetosphere, paper presented at the Chapman Memorial Sym-

- posium on Magnetospheric Motions, Boulder, Colo., June 18-22, 1973.
- Gaffey, J. D., W. B. Thompson, and C. S. Liu, Ordinary-mode electromagnetic instability for counter-streaming ions with anisotropic temperatures, part 1, *J. Plasma Phys.*, *9*, 17, 1973.
- Ginzburg, V. L., and V. V. Zheleznyakov, On the possible mechanisms of sporadic radio emission (radiation in an isotropic plasma), *Sov. Astron.*, *2*, 653, 1958.
- Gregory, P. C., Radio emission from auroral electrons, *Nature*, *221*, 350, 1969.
- Hamasaki, S., Electromagnetic micro-instabilities of plasmas in a uniform magnetic induction, *Phys. Fluids*, *11*, 2724, 1968.
- Hartz, T. R., Low frequency noise emissions and their significance for energetic particle processes in the polar ionosphere, in *The Polar Ionosphere and Magnetospheric Processes*, p. 151, Gordon and Breach, New York, 1970.
- Hasegawa, A., Heating of the magnetospheric plasma by electromagnetic waves generated in the magnetosheath, *J. Geophys. Res.*, *74*, 1763, 1969.
- Kennel, C. F., F. L. Scarf, R. W. Fredricks, J. H. McGehee, and F. V. Coroniti, VLF electric field observations in the magnetosphere, *J. Geophys. Res.*, *75*, 6136, 1970.
- Mosier, S. R., M. L. Kaiser, and L. W. Brown, Observations of noise bands associated with the upper hybrid resonance by the Imp 6 radio astronomy experiment, *J. Geophys. Res.*, *78*, 1673, 1973.
- Muldrew, D. B., Preliminary results of Isis 1 concerning electron-density variations, ionospheric resonances, and Cerenkov radiation, *Space Res.*, *10*, 786, 1970.
- Ratcliffe, J. A., *The Magneto-ionic Theory and Its Applications to the Ionosphere*, p. 59, Cambridge University Press, London, 1962.
- Shaw, R. R., and D. A. Gurnett, Magnetospheric electron density measurements from upper hybrid resonance noise observed by Imp 6, *Res. Rep. 72-37*, p. 11, Dep. of Phys. and Astron., Univ. of Iowa, Iowa City, Iowa, 1972.
- Stix, T. H., *The Theory of Plasma Waves*, p. 27, McGraw-Hill, New York, 1962.
- Stone, R. G., J. Fainberg, and L. W. Brown, Observations of traveling solar radio bursts originating between .05 and 1 AU, paper presented at the AGU Annual Fall Meeting, San Francisco, Calif., December 6-9, 1971.
- Sturrock, P. A., Spectral characteristics of type III solar radio bursts, *Nature*, *192*, 58, 1961.
- Sudan, R. N., Plasma electromagnetic instabilities, *Phys. Fluids*, *6*, 57, 1963.
- Walsh, D., F. T. Haddock, and H. F. Schulte, Cosmic radio intensities at 1.225 and 2.0 Mc measured up to an altitude of 1700 km, *Space Res.*, *4*, 935, 1964.
- Warwick, J. W., Radiophysics of Jupiter, *Space Sci. Rev.*, *6*, 841, 1967.
- Wild, J. P., Observations of the spectrum of high-intensity solar radiation at meter wavelengths, 3, Isolated bursts, *Aust. J. Sci. Res., Ser. A*, *3*, 541, 1950.

(Received May 9, 1973;
accepted August 1, 1973.)